

Effects of Epicatechin Gallate on Wound Healing and Scar Formation in a Full Thickness Incisional Wound Healing Model in Rats

Mohit Kapoor, Rowena Howard, Irene Hall, and Ian Appleton

From the Department of Pharmacology and Toxicology,
University of Otago, Dunedin, New Zealand

Catechins are naturally occurring polyphenolic compounds with putative anti-inflammatory, antioxidant and free radical scavenging effects *in vitro*. However, their potential effects *in vivo* have not been established. Therefore we have investigated the effects of the catechin epicatechin gallate (ECG), on scar formation in a full thickness incisional model of wound healing in rats. ECG showed a significant improvement in the quality of scar formation both in terms of maturity and orientation of the collagen fibers. An increase in inducible nitric oxide synthase and cyclooxygenase-2 and a decrease in arginase-I activity and protein levels were observed at earlier time points. In addition, an increase in the number of new blood vessels was observed in the ECG-treated group. This correlated with the protein levels of vascular endothelial growth factor, the most potent angiogenic protein known. This study has therefore demonstrated, for the first time, that catechins, namely ECG, can significantly improve the quality of wound healing and scar formation. These effects may in part be due to an acceleration of the angiogenic response and an up-regulation of the enzymes nitric oxide synthase and cyclooxygenase. (Am J Pathol 2004; 165:299–307)

Wound healing is a complex pathophysiological process involving interplay of several cellular and biochemical processes. This highly complex phenomenon includes the interaction of inflammation, re-epithelialization, angiogenesis, granulation tissue formation and collagen deposition.¹ Any impairment in the normal reparative process may lead to either delayed healing or excess fibrosis.² Skin ulcers, including diabetic foot ulcers, venous ulcers and pressure ulcers are among the most frequent and characteristic type of chronic non-healing wounds. One of the major causes of delayed healing is the persistence of inflammation or an inadequate angiogenic response.^{1,3} In contrast, overhealing, or excessive fibrosis of wounds is observed in fibroproliferative disorders such as keloids and hypertrophic scars. These conditions are

characterized by abnormal accumulation of collagen within the wound site as a result of failure to eliminate granulation tissue cells.² The expression of vascular endothelial growth factor (VEGF) and several enzyme systems, including nitric oxide synthase (NOS), cyclooxygenase (COX) and Arginase, are vital for maintaining the different phases of wound healing. A greater insight into the regulation, and interaction, of these enzymes and growth factors is therefore pivotal to the understanding of the normal repair process.

Catechins are naturally occurring polyphenolic compounds which have been ascribed as having anti-inflammatory, antioxidant and free radical scavenging properties *in vitro*.^{4,5} For example, epigallocatechin gallate (EGCG), one of the major isoforms of the catechins, has been shown to inhibit infiltration of leukocytes, myeloperoxidase activity and to decrease UV-B induced erythema.⁶ Catechins have also been shown to decrease the production of the pro-inflammatory cytokines IL-1 β and TNF- α and enhance the production of the anti-inflammatory cytokine, IL-10.^{7,8} It has also been reported that catechins can inhibit the production of matrix metalloproteinases.⁹ The results of *in vitro* studies hence purport to putative anti-inflammatory effects. However, the effects of catechins in *in vivo* models of inflammation and wound healing have not yet been established. We have previously demonstrated that, of the catechins, only epicatechin-3-gallate (ECG) had anti-inflammatory effects in a murine model of chronic granulomatous inflammation.¹⁰ More recently, it has been shown that ECG has the greatest antioxidant effects of all of the catechins.¹¹ Therefore, in this study we have determined the effects of ECG on wound healing and scar formation in a full thickness incisional model of dermal wound healing in rats.

Materials and Methods

Reagents

Male Sprague Dawley rats (250 ± 25 g) were obtained from Hercus Taieri Resource Unit, University of Otago, NZ. van Gieson's collagen stain and Harris's hematoxylin

Accepted for publication March 4, 2004.

Address reprint requests to Dr. Ian Appleton, Department of Pharmacology and Toxicology, University of Otago, Dunedin, P.O. Box 913, NZ. E-mail: ian.appleton@stonebow.otago.ac.nz.

from BDH (Palmerston North, NZ). Mouse anti-rat CD31 and polyclonal goat anti-human VEGF₁₆₅ from Research & Diagnostics systems (Minneapolis, MN). Bradford reagent and ECL reagents from Amersham (Auckland, NZ). Vectastain from Biotech (Auckland, NZ). Polyclonal rabbit anti-human iNOS, ecNOS and nNOS; polyclonal goat anti-human COX-1 and COX-2 from Santa Cruz Biotechnology (Santa Cruz, CA). Arginase I and II antibodies was a gift from Dr. Tomomi Gotoh (Graduate School of Medical Sciences, Kumamoto University, Japan). Arginase I antibody was raised in a rabbit by injection of recombinant human arginase I. Arginase II antibody was raised in a rabbit by injection of synthetic peptide corresponding to rat Arginase II (GenBank accession number: U90887) C-terminal portion (2791–298C). Prestained broad range kaleidoscope molecular weight markers from BioRad Laboratories (Auckland, NZ). All other chemicals were obtained from Sigma (New South Wales, AU).

Animals

Male Sprague Dawley rats (250 ± 25 g) were individually housed at 25°C and kept on a 12 hour light/dark cycle. Food and water were available *ad libitum*. All experimental procedures were in line with local ethical committee guidelines.

Full Thickness Incisional Model of Dermal Wound Healing

Twenty-four hours before wounding, animals were anesthetized with halothane, shaved and incision points marked on the dorsum. 1 cm full thickness incisional wounds were made 5 and 8 cm from the base of the neck and 2 cm from the spine to give a total of 4 wounds per animal. Wounds were left unsutured and uncovered, the animals were allowed to recover and housed individually. Animals were sacrificed by CO_2 exposure at 1, 3, 7, 14, and 21 days after wounding. Unwounded skin served as a control (day 0). For biochemical analysis the whole length of the wounds (full thickness) were carefully dissected as close to the wound margins as possible and immediately snap frozen in liquid N_2 . For histological and immunohistochemical studies an extra 5 mm of skin around all edges of each wound was dissected. Samples for histology and immunohistochemical studies were then fixed in 10% buffered formalin, then processed by graded dehydration in alcohol and then embedded in paraffin wax.

Dosing Regimen

Treatment and control groups received either 50 μl of 0.8 mg/ml of ECG or saline, respectively, intradermally, for one day prior and each day for 7 days after wounding. To minimize the possible disruption to the wound, injections were on one side then the other side of the wound on consecutive days using a 27-gauge needle.

Van Gieson's Collagen Stain and Assessment of Scarring

0.5 μm sections were cut using a microtome and collected on poly-L-lysine-coated slides. Sections were then dewaxed and rehydrated by successive immersion in descending concentrations of alcohol. To assess the effects of ECG on the quality of scarring, van Gieson's collagen stain was used. van Gieson's stain results in a deep red color for mature collagen fibers and a pink color for immature collagen fibers. Muscle and fibrin appear yellow with black nuclei. The effects of ECG on the quality of scarring at each time point, were graded on a scale of -3 to +3 by three separate blind observers. -3 signifies a worse scar in comparison to the control untreated group. This is indicated by less collagen deposition, more immature collagen fibers, disorientation of the collagen and large numbers of inflammatory cells. Whereas +3 signifies a good scar in comparison to the control, untreated group. This was indicated by more mature collagen fibers, orientation parallel to the epidermal layer, and reduced inflammatory cell numbers. Thus the more normalized the appearance of the scar in comparison to normal skin (day 0), the greater the increase in quality.

Immunohistochemical Assessment of Angiogenesis

Sections were cut and processed as above. Immunolabeling of CD31 was used as a cell surface marker of endothelial cells as we have previously described.¹² Briefly endogenous peroxide was blocked using 0.5% H_2O_2 in methanol for 30 minutes. Nonspecific IgG binding was blocked by incubating sections with normal goat serum (1:200 in PBS) for 30 minutes and then incubated with monoclonal mouse anti-rat CD31 (1:100) in a humidified chamber and left overnight at 4°C . Sections were then incubated with a biotinylated goat anti-mouse secondary antibody solution for 30 minutes followed by incubation with Vectastain enzyme conjugate for 30 minutes. The chromogen diaminobenzidine tetrahydrochloride (DAB), was then added till sufficient color development and sections counterstained with Harris's hematoxylin. Assessment of angiogenesis was carried out by three separate investigators. A score of +3 indicated large numbers of blood vessels and -3 reduced blood vessel numbers.

Tissue Preparation for Biochemical Analysis and Western Blotting

From past experience 2 wounds per animal must be pooled to give sufficient protein (minimum of 2 mg/ml) for subsequent biochemical analysis and western blotting. Tissues were homogenized using a Kinematica Polytron in a mixture of 800 μl protease inhibitors (10 $\mu\text{g ml}^{-1}$ leupeptin, 10 $\mu\text{g ml}^{-1}$ pepstatin A and 100 $\mu\text{g ml}^{-1}$ phenylmethylsulfonyl fluoride) in 50 mmol/L Tris-HCl pH 7.5. Any wound tissue adherent to the Polytron head was then washed with 200 μl of protease inhibitory buffer to

give a final volume of 1 ml. After centrifugation for 15 minutes at 2000 × g, the supernatants were used for protein determination, western blot analysis and measurement of enzyme activities. Protein levels were determined according to the method of Bradford.¹³

Assessment of Nitric Oxide Synthase Activity

Homogenates were incubated at 37°C for 30 minutes in 50 mmol/L Tris pH 7.4 containing NADPH (1 mmol/L), calmodulin (30 nmol/L), tetrahydrobiopterin (5 μmol/L), CaCl₂ (2 mmol/L), L-valine (50 mmol/L) and the substrate (a mixture of unlabelled and 10 μmol/L [³H]L-arginine). To determine the contributions of iNOS (calcium-independent) and total NOS activity (calcium-dependent), CaCl₂ was replaced with 1 mmol/L EGTA. The reaction was stopped by addition of HEPES buffer (20 mmol/L, pH 5.5) containing EDTA (1 mmol/L) and EGTA (1 mmol/L). The newly formed [³H]L-citrulline and [³H]L-arginine were then separated by passing over Dowex (mesh size ×50) chromatographic columns. Radioactivity was then assessed by liquid scintillation. Results are expressed as pmol [³H]L-citrulline/30 minutes/mg protein.

Nitrite Level Determination

Nitrite levels in the tissue homogenates were assessed using the Griess reaction method as described by Jude et al, 1999.¹⁴ Equal volumes of standard (0–100 μmol/L Na nitrite) or sample were added to the Griess reagent which consisted of equal volumes of 10 g/L sulfanilamide (in 0.5% nitrite free H₃PO₄) and 1 g/L of naphthylethylenediamine. Nitrite levels were then assessed spectrophotometrically at a wavelength of 570 nm.

Assessment of Arginase Activity

Arginase activity in the tissue homogenates was assessed using the method we have previously described.¹⁴ Briefly, to 50 μl of each sample, 50 μl of 10 mmol/L MnCl₂ in 50 mmol/L Tris-HCl (pH 7.5) was added and incubated at 55°C for 10 minutes. 25 μl of 0.5 mol/L L-arginine was added to 25 μl of the above mixture and incubated at 37°C for 1 hour. The acid mixture containing H₂SO₄, H₃PO₄ and H₂O (1:3:7) was added to stop the reaction. 9% isonitrosopropiophenone (in ethanol) was added and heated to 100°C for 45 minutes. The amount of urea formed was determined spectrophotometrically at a wavelength of 540 nm. Results are expressed as μg urea/mg protein.

Assessment of Cyclooxygenase Activity

50 μl of sample homogenate was added to 450 μl of 30 μmol/L arachidonic acid and incubated for 30 minutes at 37°C. The reaction was terminated by boiling for 7 minutes followed by centrifugation for 30 minutes at 10,000 × g. 100 μl of supernatant was incubated with anti-PGE₂ in sodium phosphate buffered saline (10 mmol/L) containing 0.1% bovine serum albumin and 0.1% sodium azide

at 4°C for 30 minutes. Samples were then incubated at 4°C with 100 μl [³H]PGE₂ for 1 hour. 1 ml ice cold dextran-coated charcoal was then added and incubated on ice for 10 minutes. This mixture was centrifuged at 2,000 × g at 4°C for 15 minutes. The amount of PGE₂ produced was measured by adding 700 μl of the resultant supernatant to 4 ml of scintillation fluid. Results are expressed as μg PGE₂/mg protein/30 minutes.

Western Blot Analysis

The protein concentrations in all samples were equilibrated to 1 mg/ml. The tissue homogenates were mixed with sample loading buffer (50 mmol/L Tris-HCl, 10% SDS, 10% glycerol, 10% 2-mercaptoethanol, 2 mg/ml bromophenol blue) in a ratio of 1:1 and then boiled for 5 minutes. Then 10 μl of each sample was loaded and separated on a 10% SDS polyacrylamide gel. The proteins were transferred to immunoblot polyvinylidene difluoride (PVDF) membranes using a transblotting apparatus (BioRad, Auckland, NZ). Membranes were incubated with 5% dried milk protein for 6 hours to block non-specific IgG binding. The membranes were then incubated overnight at 4°C with the appropriate primary antibody diluted with Tris-buffered saline (TBS). Primary antibody dilutions were as follows: iNOS, ecNOS, nNOS and VEGF₁₆₅, 1:1000; COX-1 and COX-2, 1:1500; arginase-I and arginase-II, 1:20,000. Membranes were then incubated for 6 hours at 4°C with secondary antibody as follows: ecNOS, nNOS, iNOS, and arginase I and II, horse radish peroxidase conjugated goat anti-rabbit IgG (1:1000); COX-1, COX-2 and VEGF₁₆₅, biotinylated rabbit anti-goat IgG (1:1000). For horseradish peroxidase conjugated secondary antibodies, bands were detected using the enhanced chemiluminescence (ECL) method. For biotinylated secondary antibodies bands were detected using an amplified alkaline phosphatase kit and developed with 5-bromo-4-chloro-3-indolylphosphate as the chromogen. Molecular weight was determined with prestained broad range kaleidoscope markers. The density of bands was scanned and quantified using BioRad Quantity One software. Results for COX-1, COX-2 and VEGF are expressed as relative density. All others are expressed as optical density.

Statistical Analysis

Statistical analysis was performed using a 2-tailed analysis of variance (ANOVA) test in conjunction with a post hoc Mann-Whitney U-test. Results are expressed as the mean ± SEM (SEM) for n = 5–8 separate observations. P < 0.05 was considered statistically significant (*).

Results

Effect of ECG on Scar Formation (Blind Histological Study)

van Gieson's collagen stain demonstrated that in the day 21 ECG-treated group, the collagen fibers within the

wound site were compact, more mature (red to deep red color) and orientated parallel to the epidermal layer (Figure 1b). In contrast, in the control group collagen fibers within the wound site were less compact, immature (pale pink color) and disorientated (Figure 1a). Semiquantitative analysis, by blind histological investigation, showed that the ECG-treated group had a significant improvement in the quality of the scar on day 14 ($P < 0.05$) and significant improvement on day 21 ($P < 0.01$), after wounding (Figure 1c).

Effect of ECG on New Blood Vessel Formation

Blind immunohistochemical study using the endothelial cell marker CD31 (platelet endothelial cell adhesion molecule or PECAM) showed that the ECG-treated group had a significant effect on new blood vessel formation. The ECG-treated group showed a significant increase in the number of blood vessels at the wound site on days 1 ($P < 0.01$) and 3 ($P < 0.05$), peaking at day 1 (Figure 2, b and c). Whereas by day 7, and later time points, few blood vessels were observed in the ECG-treated group. In contrast, few new blood vessels were observed on day 1 in the control group (Figure 1a). The number of new blood vessels in the control group reached a significant peak at day 7 ($P < 0.05$). Thus, treatment with ECG resulted in an acceleration of new blood vessel formation.

VEGF₁₆₅ Expression

The levels of VEGF protein paralleled the profile of blood vessel formation in both controls and the ECG-treated group. VEGF₁₆₅ was detected at a MW of 23 kd (Figure 3a). Quantification of the protein levels of VEGF₁₆₅ showed a significant up-regulation of VEGF₁₆₅ protein levels, in the ECG-treated group, on days 1 ($P < 0.01$) and 3 ($P < 0.05$), peaking at day 3 and thereafter returning to basal levels (Figure 3b). In the control group, protein levels of VEGF₁₆₅ were significantly lower on days 1 and 3 but were significantly higher on day 7 ($P < 0.01$) compared to the ECG group.

Effect of ECG on NOS Activity and NOS Isoform Protein Levels

In both the control and ECG-treated groups iNOS activity (in the absence of calcium) accounted for virtually all of the total NOS activity (data not shown). iNOS activity showed a significant up-regulation in the ECG-treated group on days 1 ($P < 0.01$), 3 ($P < 0.05$) and 7 ($P < 0.05$), peaking at day 3 and then returning to basal levels at the later time points (Figure 4b). Analysis of NOS isoform (ecNOS, nNOS and iNOS) protein levels, assessed by western blot analysis, correlated with activity data, in that most of the NOS activity was attributed to the inducible isoform. No change in the protein levels of nNOS and ecNOS were observed (data not shown). The iNOS protein band was observed at a MW of approximately 130 kd (Figure 4a).

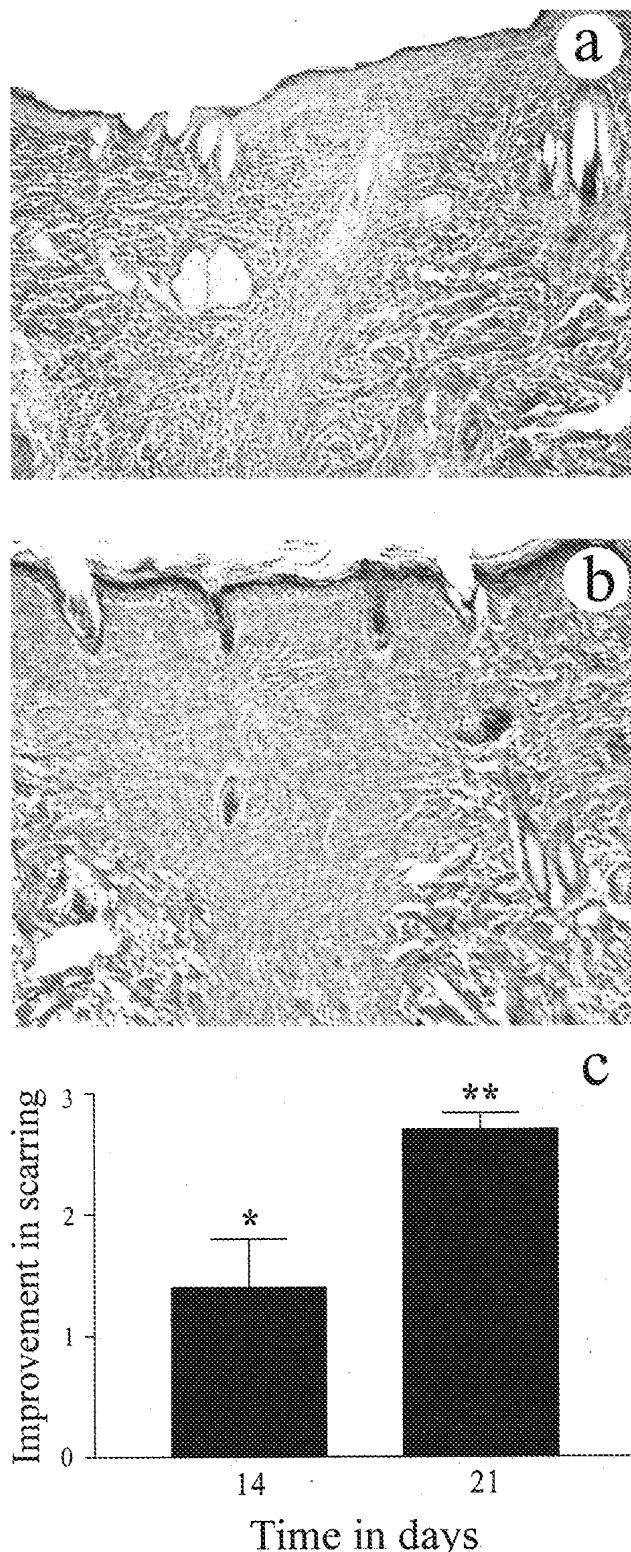


Figure 1. The effects of ECG on scar formation using van Gieson's collagen stain. ECG showed a significant improvement in the quality of the scar at 21 days after wounding. ECG-treated group (b) showed more compact collagen deposition, greater maturity of collagen fibers, and the orientation of collagen fibers was parallel to the epidermis compared to the control group (a). Blind histological analysis (scale of -3 to +3) showed significant differences in the quality of the scar between the groups on days 14 ($P < 0.05$) and 21 ($P < 0.01$; c). Each bar represents the mean \pm SEM for $n = 5$ separate observations. * $P < 0.05$ and ** $P < 0.01$. Magnification, $\times 6.3$.

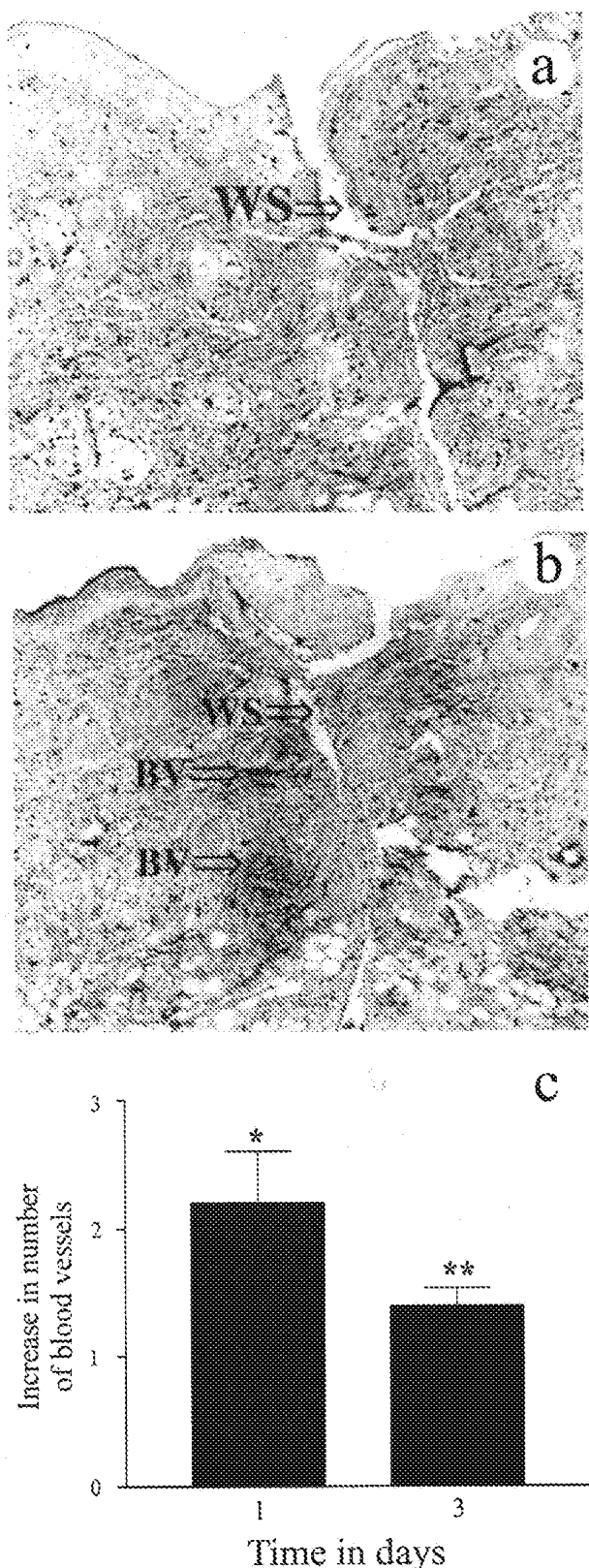


Figure 2. The effects of ECG on new blood vessel formation using the endothelial cell marker CD31. The ECG-treated group (**b**) showed a significant increase in the number of blood vessels on day 1 after wounding compared to the control group (**a**). Blind analysis (**c**) showed a significant increase in the number of blood vessels on days 1 ($P < 0.01$) and 3 ($P < 0.05$) in the ECG group compared to the controls. Each bar represents the mean \pm SEM for $n = 5$ separate observations. * $P < 0.05$ and ** $P < 0.01$. WS, wound site; BV, blood vessels. Magnification, $\times 6.3$.

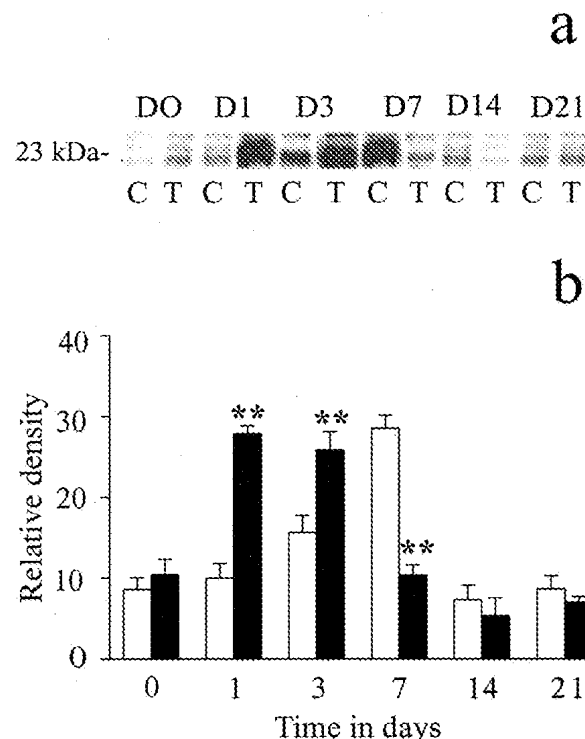


Figure 3. The effects of ECG on VEGF₁₆₅ protein levels. Western blot analysis showed significant up-regulation of VEGF₁₆₅ protein levels in ECG-treated group (**closed bars**) on days 1 and 3 (both $P < 0.01$) compared to the control group (**open bars**; **a** and **b**). By day 7, the end of the treatment regimen, the ECG levels had significantly reduced ($P < 0.01$) back to basal levels. In **a**, C represents the control group and T represents the ECG-treated group. D0 to D21 represents the time course of study. Each point represents the mean \pm SEM for $n = 5$ different observations. ** $P < 0.01$.

Effect of ECG on Nitrite Levels

The levels of nitrite (as determined by the Griess reaction) in both the control and ECG-treated groups mirrored that of iNOS activity. The ECG-treated group showed a significant increase in nitrite levels at days 1 ($P < 0.05$) and 3 ($P < 0.05$; Figure 4d).

Effect of ECG on COX Activity and COX Isoform Protein Levels

COX activity showed a significant increase in the ECG-treated group on days 1 ($P < 0.01$), 3 ($P < 0.05$) and 7 ($P < 0.01$), peaking at day 3 and then returning to basal levels at the later time points (Figure 5b). COX protein levels (COX-1 and COX-2), assessed by western blot analysis, showed that most of the COX activity was attributed to the inducible isoform, COX-2. No change in the protein levels of COX-1 were observed (data not shown), whereas COX-2 protein levels exhibited a similar profile as the activity data. The COX-2 protein band was observed at a MW of approximately 70 kd (Figure 5a).

Effect of ECG on Arginase Activity and Arginase Isoform Protein Levels

A significant decrease in arginase activity was observed in the ECG-treated group on days 1 ($P < 0.05$) and 3

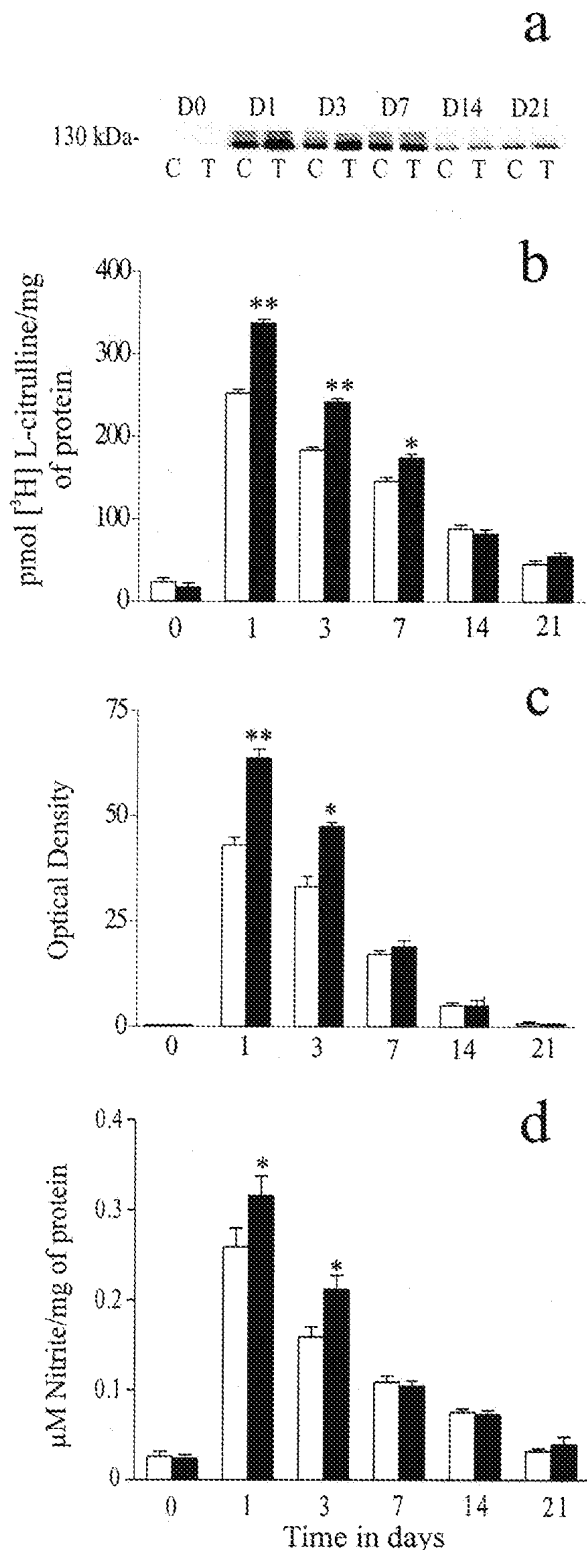


Figure 4. The effects of ECG on iNOS protein levels (**a** and **c**) and activity (**b**). The ECG-treated group showed a significant increase in iNOS activity on days 1 ($P < 0.01$), 3 ($P < 0.01$) and 7 ($P < 0.05$; **b**). Western blot analysis (**a** and **c**) showed a significant up-regulation of iNOS protein levels on days 1 ($P < 0.01$) and 3 ($P < 0.05$) in the ECG-treated group. A significant increase in nitrite levels was observed in the ECG-treated group on days 1 ($P < 0.05$) and 3 ($P < 0.05$; **d**). In the graphs, **open bars** represent the control group and **closed bars** represent the ECG-treated group. In **a**, C represents the control group and T represents the ECG-treated group. D0 to D21 represents the time course of study. In the graphs, **open bars** represent the control group and **closed bars** represent the ECG-treated group. In **a**, C represents the control group and T represents the ECG-treated group. D0 to D21 represents the time course of study. Each point represents the mean \pm SEM for $n = 5$ to 8 separate observations. * $P < 0.05$; ** $P < 0.01$.

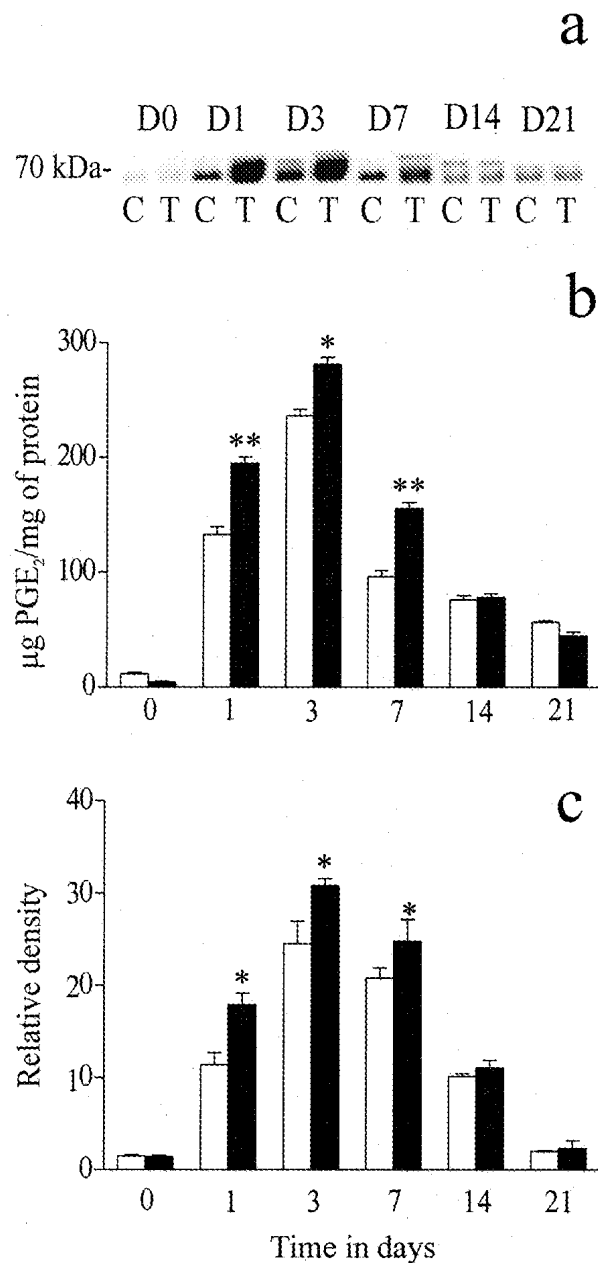


Figure 5. The effects of ECG on COX-2 protein levels (**a** and **c**) and COX activity (**b**). The ECG-treated group showed a significant increase in COX activity on days 1 ($P < 0.01$), 3 ($P < 0.05$) and 7 ($P < 0.01$; **b**). Western blot analysis showed a significant up-regulation of COX-2 protein levels on days 1, 3, and 7 (all $P < 0.05$) in the ECG-treated group (**a** and **c**). In **a**, C represents the control group and T represents the ECG-treated group. D0 to D21 represents the 21-day time course of study. In the graphs, **open bars** represent the control group and **closed bars** represent the ECG-treated group. Each point represents the mean \pm SEM for $n = 5$ to 8 separate observations. * $P < 0.05$; ** $P < 0.01$.

($P < 0.01$) compared to the controls (Figure 6b). Arginase protein levels (arginase-I and arginase-II), assessed by western blot analysis, showed that virtually all of the arginase activity was attributed to the arginase-I isoform. No protein bands for arginase-II were observed (data not shown), whereas arginase-I showed a similar protein expression profile as the activity data. The arginase-I protein band was observed at MW of approximately 70 kd (Figure 6a).

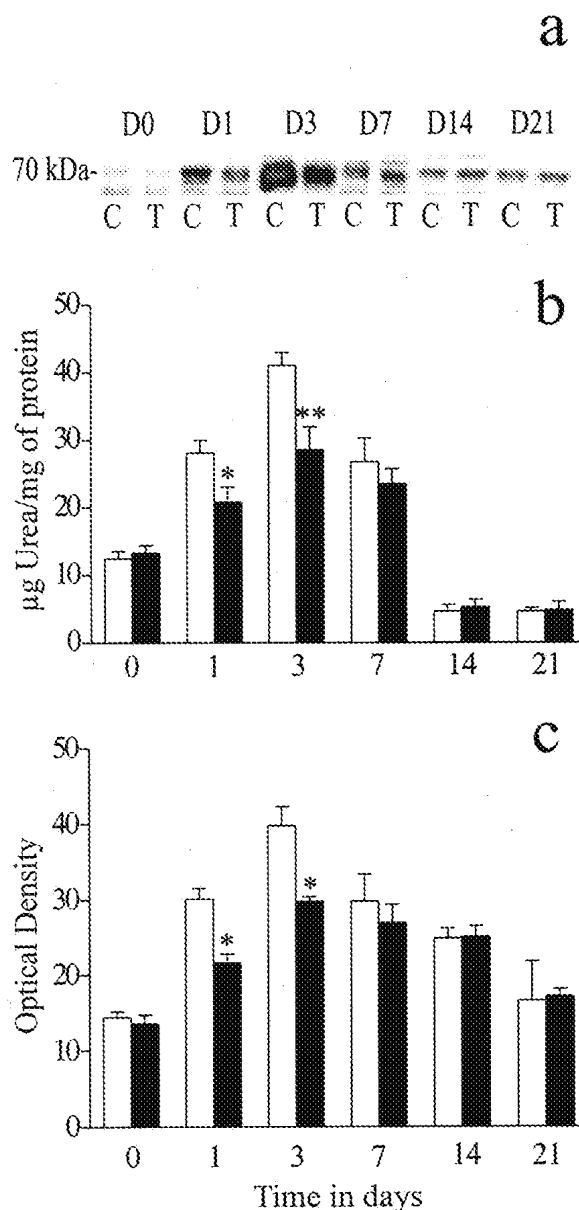


Figure 6. The effects of ECG on arginase-II protein levels (**a** and **c**) and arginase activity (**b**). The ECG-treated group showed a significant decrease in arginase activity on days 1 ($P < 0.05$) and 3 ($P < 0.01$; **b**). Western blot analysis showed a significant down-regulation of arginase-II protein levels on days 1 and 3 (both $P < 0.05$) in the ECG-treated group (**a** and **c**). In **a**, C represents the control group and T represents the ECG-treated group. D0 to D21 represents the time course of study. In the graphs, open bars represent the control group and closed bars represent the ECG-treated group. Each point represents the mean \pm SEM for $n = 5$ to 8 separate observations. * $P < 0.05$; ** $P < 0.01$.

Discussion

An alteration in the sequence of wound healing may result in the development of an abnormal wound, leading to either delayed healing or excessive fibrosis.¹⁵ The most common examples of delayed healing include diabetic foot ulcers, venous leg ulcers and pressure ulcers. Overhealing is observed in fibroproliferative disorders such as hypertrophic scars and keloids, which are characterized by excessive accumulation of collagen fibers within the wound site.¹⁶ The regulation of several enzyme

systems and growth factors is vital for normal wound healing. These include NOS, COX, arginase, and VEGF.¹⁷⁻²⁰ Catechins have antioxidant and free radical scavenging effects and there is compelling evidence of their possible anti-inflammatory effects.^{4,5} All these potential effects have been described in *in vitro* studies but their potential effects in *in vivo* studies are still not known.

The quality of scarring is a vital indicator of the normal wound healing process. We have demonstrated, using van Gieson's collagen stain, that treatment with ECG results in a significant improvement in the quality of scarring, both in terms of collagen orientation and maturity. Moreover, the collagen fibers within the wound site were observed to be more compact compared to the control group (Figure 1). In addition, we have investigated the potential biochemical mechanisms responsible for this observation.

Wound healing is an angiogenesis dependant process, as oxygen and nutrients are required to promote the newly forming granulation tissue.²⁰ During normal wound healing, new blood vessel formation begins within 3 days, peaks at day 7, and thereafter resolves, resulting in the characteristic avascular scar. Blind immunohistochemical analysis using the endothelial cell marker CD31, showed that in the ECG-treated group, a significant number of new blood vessels started to appear at day 1. After day 7, almost no blood vessels were discerned. ECG treatment, therefore, resulted in an acceleration of the normal angiogenic response and wound healing.

Vascular endothelial growth factor is the most potent angiogenic factor yet discovered.²¹ We therefore investigated the effects of ECG on VEGF levels. Western blot analysis showed that ECG treatment resulted in a significant up-regulation of VEGF protein expression at days 1 and 3. Thereafter the levels declined to basal (Figure 3). This mirrored the immunohistochemical profile of new blood vessel development. This observation further confirms the pivotal role VEGF plays in angiogenesis. VEGF expression has been closely linked to two of the classical enzymes involved in inflammation and wound healing, namely COX and NOS.^{22,23} Therefore to further characterize the mechanisms of the effects of ECG we studied COX and NOS activity and the expression of their protein levels.

L-Arginine is metabolized by several enzyme systems including NOS. L-Arginine when metabolized by NOS results in the production of NO and L-citrulline.²⁴ ECG treatment showed a significant increase in NOS activity at earlier time points. This increase was almost exclusively due to the inducible isoform, iNOS. Western blot analysis confirmed that virtually all NOS activity was attributed to iNOS with no change in the expression of nNOS and eNOS. We also determined the effects of ECG on nitrite, the stable breakdown product of NO. ECG treatment resulted in a significant increase in nitrite levels on days 1 and 3; an almost identical profile to iNOS activity. Recent studies have shown that NO derived from iNOS is vital for wound repair.²⁵ NO derived from iNOS has also been closely linked to VEGF expression and angiogenesis. NO derived from iNOS increases the expression of

VEGF during cutaneous wound healing.²⁵ Furthermore, NO has been shown to increase VEGF mediated endothelial cell migration.²⁶ Also, it has been reported that fibroblasts derived from iNOS knockout mice have slower rates of proliferation and decreased collagen synthesis.²⁷ NO derived from iNOS is therefore critical for wound collagen synthesis and in acquiring mechanical strength. This is further confirmed by a study which reported that inhibition of iNOS significantly decreased wound fibroblast collagen synthesis.²⁸ More recently, iNOS has been shown to also have an anti-fibrotic role.²⁹ Furthermore it was shown that, iNOS inhibition resulted in a decrease in the ratio of NO:ROS (reactive oxygen species) with a resultant increase in collagen deposition and fibrosis. Thus induction of iNOS may be one of the protective mechanisms against fibrosis and abnormal wound healing. NO derived from iNOS has also been shown to have cytostatic activity with a net increase in collagen synthesis.³⁰ Thus the finding that ECG caused an increase in iNOS activity, and hence NO, could have resulted in increased cytostatic activity, accelerated collagen deposition and an up-regulation of VEGF. This might, in part, be one of the mechanisms through which ECG showed a significant improvement in wound healing and scar formation.

Cyclooxygenase is another classical enzyme involved in inflammation and wound repair. COX catalyzes the conversion of arachidonic acid to prostaglandins (PGs) and thromboxanes (TXs). COX contributes to the process of inflammation, cellular proliferation and neovascularization through the production of prostanoids. The major prostaglandin formed during inflammation is PGE₂ (for review of COX in inflammation see reference 18). In this study, the ECG-treated group showed a significant increase in COX activity, which was almost exclusively attributable to the inducible isoform, COX-2. COX-2 has been reported to also have possible anti-inflammatory properties.³¹ Recently, it was proposed that the COX-2 isoform may have pro-inflammatory action during the early inflammatory phase but it might help in the resolution of inflammation later on by generating anti-inflammatory prostaglandins.³¹ Also COX and PGE₂ have shown to be more important in the early stages of wound healing by promoting fibrosis and decreasing the accumulation of macrophages within the wound site.³² PGE₂ has been reported to be involved in proliferation of fibroblasts and the promotion of collagen synthesis at earlier time points during wound healing.³³ VEGF up-regulation is linked to COX-2 expression and activity. This is illustrated by the finding that COX-2 inhibition, inhibits the expression of VEGF and angiogenesis.²² Furthermore, PGE₂ can stimulate VEGF expression in cultured osteoblasts and fibroblasts.^{34,35} Therefore, the observation that ECG treatment caused an increase in COX-2 and VEGF expression, in conjunction with up-regulation of iNOS, might be another contributing factor for the accelerated rate of angiogenesis in the ECG group at the earlier time points.

In addition to NOS, L-arginine can also be metabolized by the enzyme arginase with the resultant production of L-ornithine and urea.^{36,37} L-Ornithine is further converted

to the polyamines (involved in cell growth and differentiation) and proline, the building block for collagen synthesis.³⁸ In this study, ECG treatment resulted in a significant decrease in arginase activity at the early time points. Arginase activity was solely due to the arginase-I isoform. The arginase I isoform was recently reported to be up-regulated in wound derived fibroblasts while arginase II levels were not detectable.³⁹ Increased levels of arginase activity have been found in keloids and this could account for the characteristic excessive collagen accumulation observed in this condition (I. Appleton, unpublished observations). Thus, the reduction in arginase activity might account for the more normalized appearance of the scar observed with ECG treatment. It is important to emphasize that a scar is basically an acellular mass of collagen. Any reduction in collagen deposition at later time points would be beneficial as this would more closely resemble the surrounding normal dermal architecture. However, ECG treatment did not completely inhibit arginase activity. This suggests that the attenuation of arginase activity by ECG might be sufficient for normal wound healing but not enough to produce excess collagen deposition and therefore a severe scar.

The results of this study have demonstrated, for the first time, that treatment with ECG results in a significant improvement in wound healing and the quality of scarring. In addition, we have elucidated the possible biochemical mechanisms involved in this process.

Acknowledgments

We thank Dr. Tamomi Gotoh for providing arginase I and arginase II antibody. Special thanks to Dr. Ping Liu for technical advice.

References

- Appleton I: Wound healing: future directions. *Invest Drugs* 2003, 6:1067–1072
- Desmouliere A, Redard M, Darby I, Gabiani G: Apoptosis mediates the decrease in cellularity during the transition between granulation tissue and scar. *Am J Pathol* 1995, 146:1029–1039
- Norrbj K: Angiogenesis: new aspects relating to its initiation and control. *Acta Pathol Microbiol Immunol Scand* 1997, 105:417–437
- Chan MM-Y, Dunne F, Ho C-T, Huang H-I: Inhibition of inducible nitric oxide synthase gene expression and enzyme activity by epigallocatechin gallate, a natural product from green tea. *Biochem Pharmacol* 1999, 54:1281–1286
- Yen GC, Chen HY: Scavenging effect of various tea extracts on superoxide derived from the metabolism of mutagens. *Biosci Biotech Biochem* 1998, 62:1768–1770
- Katiyar SK, Matsui MS, Elmetts CA, Mukhtar H: Polyphenolic antioxidant epigallocatechin-3-gallate from green tea reduces UVB-induced inflammatory responses and infiltration of leukocytes in human skin. *Photochem Photobiol* 1999, 69:148–153
- Yang F, de Villiers WJ, McClain CJ, Varilek GW: Green tea polyphenols block endotoxin-induced tumor necrosis factor-production and lethality in a murine model. *J Nutr* 1998, 128:2334–2340
- Crouvezier S, Powell B, Keir D, Yaqoob P: The effects of phenolic components of tea on the production of Pro- and anti-inflammatory cytokines by human leukocytes *in vitro*. *Cytokine* 2000, 13:280–286
- Isemura M, Saeki K, Minami T, Hayakawa S, Kimura T, Shoji Y, Suzaku M: Inhibition of matrix metalloproteinases by tea catechins and related polyphenols. *Ann NY Acad Sci* 1999, 30:629–631

10. Frampton L, Rahman R, Bolger C, Hall I, Appleton I: The effects of catechins on a murine model of chronic granulomatous inflammation. Proceedings of the Australian Health Medical Research Congress, Melbourne, National Health and Medical Research Council, November 25–29, 2002, p 2030
11. Caturla N, Vera-Samper Villalain J, Reyes Mateo C, Micol V: The relationship between the antioxidant and the antibacterial properties of galloylated catechins and the structure of phospholipid model membranes. *Free Rad Biol Med* 2003, 34:648–662
12. Appleton I, Brown NJ, Willis D, Colville-Nash PR, Alam C, Brown JR, Willoughby DA: The role of vascular endothelial growth factor in a murine chronic granulomatous tissue air pouch model of angiogenesis. *J Pathol* 1996, 180:90–94
13. Bradford MM: A rapid and sensitive method for the quantitation of microgram quantities of protein utilising the principle of protein-dye binding. *Ann Biochem* 1979, 72:248–254
14. Jude E, Boulton A, Ferguson MWJ, Appleton I: The role of nitric oxide synthase and arginase in diabetic foot ulceration: modulatory effects of transforming growth factor beta. *Diabetologia* 1999, 42:748–757
15. Greenhalgh DG: The role of apoptosis in wound healing. *Int J Biochem Cell Biol* 1998, 30:1019–1030
16. Tredget EE, Nedelec B, Scott PG, Ghahary A: Hypertrophic scars, keloids, and contractures: the cellular and molecular basis for therapy. *Surg Clin North Am* 1997, 77:701–730
17. Most D, Efron DT, Shi HP, Tantry US, Barbul A: Characterisation of incisional wound healing in inducible nitric oxide synthase knockout mice. *Surgery* 2002, 132:866–876
18. Appleton I, Tomlinson A, Willoughby DA: Induction of cyclooxygenase and nitric-oxide synthase in inflammation. *Adv Pharmacol* 1996, 35:27–78
19. Abd-EI-Aleem S, Ferguson MWJ, Appleton I, Kairsingh S, Jude E, Jones K, McCollum C, Ireland G: Expression of nitric oxide synthase isoforms and arginase in normal human skin and chronic venous leg ulcers. *J Pathol* 2000, 191:434–442
20. Folkman J, Shing Y: Angiogenesis: a mini review. *J Biol Chem* 1992, 267:10931–10934
21. Ferrara N: Vascular endothelial growth factor and the regulation of angiogenesis. *Rec Prog Horm Res* 2000, 55:15–35
22. Gallo O, Franchi A, Magnelli L, Sardi I, Vannacci A, Boddi V, Dharug V, Masianni E: Cyclooxygenase-2 pathway correlates with VEGF expression in head and neck cancer. Implications for tumor angiogenesis and metastasis. *Neoplasia* 2001, 3:53–61
23. Frank S, Kampfer H, Weitzler C, Pfeilschifter J: Nitric oxide drives skin repair: novel functions of an established mediator. *Kidney Int* 2002, 61:882–888
24. Zhang J, Snyder SH: Nitric oxide in the nervous system. *Annu Rev Pharmacol Toxicol* 1995, 35:213–233
25. Frank S, Stallmeyer B, Kampfer H: Nitric Oxide triggers enhanced induction of vascular endothelial growth factor expression in cultured keratinocytes (HaCaT) and during cutaneous wound repair. *FASEB J* 1999, 13:2002–2014
26. Noiri E, Lee E, Testa J, Quigley J, Cofflesh D, Keese CR, Giaevers I, Goligorsky MS: Podokinesis in endothelial cell migration: role of nitric oxide. *Am J Physiol* 1998, 247:C236–C244
27. Shi HP, Efron DT, Most D, Barbul A: The role of iNOS in wound healing. *Surgery* 2001, 130:225–229
28. Schaffer MR, Efron PA, Thorton FJ: Nitric oxide: an autocrine regulator of wound fibroblast synthetic function. *J Immunol* 1997, 158:2375–2381
29. Ferrini MG, Vernet D, Magee TR, Shahed A, Qian A, Rajfer J, Gonzalez-Cadavid NF: Antifibrotic role of inducible nitric oxide synthase. *Nitric Oxide Biol Chem* 2002, 6:283–294
30. White MB, Thorton FJ, Efron DT: Enhancement of fibroblast collagen synthesis by nitric oxide. *Nitric Oxide* 2000, 4:572–582
31. Gilroy DW, Colville-Nash PR, Willis D, Chivers J, Paul-Clark MJ, Willoughby DA: Inducible cyclooxygenase may have anti-inflammatory properties. *Nat Med* 1999, 5:698–701
32. Talwar M, Moyana TN, Bharadwaj B, Tan LK: The effect of a synthetic analogue of prostaglandin E₂ on wound healing in rats. *Ann Clin Lab Sci* 1996, 26:451–457
33. Sanchez T, Moreno JJ: Role of phospholipase A (2) in growth-dependent changes in prostaglandin release from 3T3 fibroblasts. *J Cell Physiol* 2001, 189:237–243
34. Harada S, Nagy JA, Sullivan KA, Thomas KA, Endo N, Rodan GA, Rodan SB: Induction of vascular endothelial growth factor expression by prostaglandin E₂ and E₁ in osteoblasts. *J Clin Invest* 1994, 93: 2490–2496
35. Ben-Av P, Crofford LJ, Wilder RL, Hla T: Induction of vascular endothelial growth factor expression in synovial fibroblasts by prostaglandin E and interleukin-1 A potential mechanism of inflammatory angiogenesis. *FEBS Lett* 1995, 372:83–87
36. Wiesinger H: Arginine metabolism and the synthesis of nitric oxide in the nervous system. *Prog Neurobiol* 2001, 64:365–391
37. Wu G, Morris SM: Arginine metabolism: nitric oxide and beyond. *Biochem J* 1998, 336:1–17
38. Hui Li, Cynthia J, Meininger, James R. Hawker Jr, Tony E Haynes, Diane Kepka-Lenhart, Sanjay K Mistry, Sidney M Morris Jr, and Guoyao Wu: regulatory role of arginase I and II in nitric oxide, polyamine, and proline syntheses in endothelial cells *Am J Physiol Endocrinol Metab* 2001, 280:E75–E82
39. Witte M, Barbul A, Schick M, Vogt N, Becker HD: Upregulation of arginase expression in wound-derived fibroblasts. *J Surg Res* 2002, 105:35–42